SIAM J. APPL. MATH.
Vol. 54, No. 3, pp. 708–730, June 1994

007

THE EFFECT OF MICROSTRUCTURE ON ELASTIC-PLASTIC MODELS*

LIANJUN AN† AND ANTHONY PEIRCE†

Abstract. For large deformations, the governing equations of elastic-plastic flow may lose their hyperbolicity and become ill posed at some critical values of the hardening modulus. This ill-posedness is characterized by uncontrolled growth of the amplitude of plane wave solutions in certain directions. To capture post-critical behavior, microstructure is built into the constitutive relations. Two types of microstructure are included: one accounts for intergranular rotation via Cosserat theory, and the other accounts for the formation of voids at the microscale by means of a new pressure term related to the gradient of the dilational deformation. Using both a linearized analysis and integral estimates, it is shown that the microstructure terms provide regularizing mechanisms that inhibit the occurrence of both shear band ill-posedness and flutter ill-posedness. Moreover, a local analysis shows that the problem can be reduced to two turning point singular Schrödinger equations in the neighborhood of points where the equations reach the critical value of the hardening modulus. Using matched asymptotics and Wentzel–Kramers–Brillouin (WKB) theory, a relation is derived between the thickness of the localization (internal layer) and the internal length scale of the material introduced by the microstructure terms

Key words. ill posed equations, granular material, the flutter instability, shear banding, shear strain hardening, loss of hyperbolicity, singular perturbation

AMS subject classifications. 35B25, 35M05, 73E99, 73H10

Introduction. The governing equations describing the deformation of elastic-plastic materials become ill posed when the accumulation of plastic deformation reaches certain critical values. A linear analysis of simple models based on the classical theory of plasticity successfully predicts the onset of ill-posedness [1], [7], [10], [11], however, it fails to track the post-critical behavior of the solution. In this paper we investigate how the inclusion of microstructure influences the behavior of solution, especially in the post-critical regime.

The ill-posedness predicted by the linear analysis is direction-dependent and is characterized by uncontrolled growth of the amplitude of plane wave solutions in certain directions. At the onset of ill-posedness [1], [7], deformation takes place in localized regions at the grain size level. This is corroborated by experimental evidence that demonstrates that shear bands in granular materials involve a number of grains. Classical theories of plasticity fail to predict deformation in the post-critical regime because an internal length scale is not built into these constitutive relations. Numerical models based on these constitutive laws choose the mesh size as their natural post-critical length scale and yield undesirable solutions in which failure patterns are dependent on the mesh size chosen for the analysis.

To capture post-critical behavior, researchers have included some form of microstructure into their models. The microstructure phenomena are typically represented by terms in the governing equations involving higher order gradients of the strain rate and rotation rate tensors. In [9], Mühlhaus and Vardoulakis incorporated

*Received by the editors October 13, 1992; accepted for publication (in revised form) August 3, 1993. This work was supported by the National Scieces and Engineering Research Council of Canada.

† Department of Mathematics and Statistics, McMaster University, Hamilton, Ontario, Canada L8S 4K1 (anthony@icarus.math.mcmaster.ca).

microstructure into a deformation theory description by accounting for intergranular slip and rotation using Cosserat theory, which resulted in additional terms in the governing equations involving the gradient of rotation. Later Vardoulakis and Aifantis [14] modified the deformation theory to incorporate microstructure into the model by including terms involving the gradient of the total shear strain. Applying a bifurcation analysis to these models and using experimental data they were able to derive a relation between the thickness of the shear band and the grain size.

In our paper we consider a plasticity model that incorporates microstructure accounting for both intergranular rotation and the formation of voids at the microscale. To account for the intergranular rotation, we adopt the simplified version of Cosserat theory introduced by Mindlin and Tiersten [8], while the voiding is modeled by a new pressure term that is related to the gradient of the dilational deformation. We believe that this model maintains the essential features of microstructure for the materials we wish to model. We show that both the Cosserat theory and the new pressure term have a dispersive effect that serve to regularize solution in the rotational and dilational directions, respectively. By performing a local analysis in a neighborhood of the regions in which equations become ill-posed, it is possible to approximate the governing equations by time-independent singular Schrödinger equations in which the potentials (in the quantum mechanical sense) have two turning points that are associated with the boundaries of the region of ill-posedness. The Schrödinger equations are singular in the sense that the highest derivatives are multiplied by a small parameter. Making use of classical WKB theory and leading order matched asymptotics we can obtain a relation between the thickness of localization region and the internal length scale of the material.

This paper is organized as follows. In §1, we introduce the microstructure terms and discuss the governing equations. In §2, we review previous work and derive conditions under which the equations become shear band ill posed and when the equations become flutter ill posed. In §3, we use linearized analysis and integral estimates to show how microstructure affects the behavior of the solution. In §4, we use local analysis to reduce the problem to a two turning point singular Schrödinger equation and use WKB theory to derive the relation between the thickness of localization and the internal length scale of the material. In §5 we summarize the results of this paper and make some concluding remarks. For the convenience of the reader, we include two appendices. In Appendix A, we derive the energy estimates that exploit the theory of pseudo differential operators. In Appendix B, we derive the matching condition by using WKB theory and matched asymptotics for a nonstandard two turning point problem that arises in the analysis of a nongeneric situation that occurs in this paper.

1. Microstructure and the governing equations.

1.1. Formulation of the problem. In this paper we consider an elastic-plastic material in which microscale rotational effects (e.g., due to slip between grains) are modeled by a continuum description using Cosserat theory and microscale dilation effects (e.g., due to microscale voiding) that are modeled by introducing a new pressure term into the constitutive relations. The summation convention is assumed unless specified.

The unknowns consist of the density ρ, the Cauchy stress T, the couple stress S, and velocity v. The conservation of mass can be expressed in the form

$$d_t\rho + \rho\partial_j v_j = 0, \tag{1.1}$$

where $d_t = \partial_t + v_j \partial_j$ is the material derivative. The conservation of momentum can be expressed in the form

$$\rho d_t v_j + \partial_i T_{ij} = 0. \tag{1.2}$$

The conservation of angular momentum can be expressed in the form

$$\partial_k S_{kl} = e_{lmn} T_{mn} = e_{lmn} T^{(a)}_{mn}, \tag{1.3}$$

where e_{lmn} is the alternating tensor with $e_{123} = 1$ and $T^{(a)}_{mn}$ is the antisymmetric part of the Cauchy stress T. Inclusion of the couple stress S is due to the Cosserat theory and, as a result, the Cauchy stress T is not symmetric.

To formulate the constitutive relations, we decompose the Cauchy stress T into three parts:

$$T_{ij} = T^{(s)}_{ij} + T^{(a)}_{ij} + p\delta_{ij}, \tag{1.4}$$

where $T^{(a)}$ is defined in (1.3), $T^{(s)}$ is a symmetric tensor, and the third term is the dispersive pressure, which accounts for the effect of microscale voids opening in the material. We also decompose the strain rate tensor

$$V_{ij} = -\frac{1}{2}\left(\partial_i v_j + \partial_j v_i\right) \tag{1.5}$$

into elastic and plastic parts

$$V = V^{(e)} + V^{(p)}. \tag{1.6}$$

Note that the minus sign in (1.5) corresponds to the convention that the compressive stresses are positive.

For $V^{(e)}$, we assume the linear strain-stress relation

$$V^{(e)}_{ij} = C_{ijkl} \nabla_t T^{(s)}_{kl}, \tag{1.7}$$

where C is a fourth-order tensor whose inverse E can be expressed through the shear modulus G and Poisson's ratio ν

$$E_{ijkl} = \frac{2\nu G}{1-2\nu}\delta_{ij}\delta_{kl} + G\left(\delta_{ik}\delta_{jl} + \delta_{il}\delta_{jk}\right). \tag{1.8}$$

To get an objective measure of the rate of change of stress, we use the Jaumann corotational rate

$$\nabla_t T^{(s)}_{kl} = d_t T^{(s)}_{ij} - T^{(s)}_{ik}\omega_{kj} - T^{(s)}_{jk}\omega_{ki},$$

where

$$\omega_{kl} = \frac{1}{2}\left(\partial_k v_l - \partial_l v_k\right)$$

is the spin rate tensor.

For the plastic part $V^{(p)}$, we assume that

$$V^{(p)}_{ij} = \frac{1}{h}\Psi_{ij}\Phi_{kl}\nabla_t T^{(s)}_{kl}. \tag{1.9}$$

The scalar h is the plastic hardening modulus, which changes from $+\infty$ to 0 as plastic deformations are accumulated. The symmetric tensor Ψ, which defines the flow rule, indicates the direction of plastic deformation in stress space. The symmetric tensor Φ is the normal direction to the yield surface (the gradient of the yield function with respect to stresses). For convenience, we normalize Ψ and Φ in the sense that

$$|\Psi^{(d)}| = |\Phi^{(d)}| = 1,$$

where for $n \times n$ matrices $\{A_{ij}\}$, the deviator and the norm of A are defined as

$$A^{(d)} = A - \frac{1}{n}\operatorname{tr}(A)I, \qquad |A|^2 = \frac{1}{2}A_{ij}A_{ij}.$$

We can write Ψ and Φ as

$$\Psi_{ij} = \Psi_{ij}^{(d)} - \beta\delta_{ij}, \qquad \Phi_{ij} = \Phi_{ij}^{(d)} - \mu\delta_{ij}.$$

In practice, Ψ and Φ might depend on loading history as well as on the current state of stress. The parameter μ specifies the angle of internal friction of the material and β specifies the amount of dilation. Typically, we assume that

$$1 > \mu > \beta > 0.$$

The flow rule is said to be deviatorically associative if and only if $\Psi^{(d)} = \Phi^{(d)}$. See [1] for a derivation of (1.9) and a physical description of its terms in greater detail.

We can replace $T^{(s)}$ by $T^{(s)} + T^{(a)}$ in (1.7) and (1.9). In fact, the antisymmetric part of T does not make a contribution since C in (1.7) is symmetric with respect to the second two indices and Φ in (1.9) is a symmetric tensor.

In the form of Cosserat theory considered here, which is an extension of linear elasticity, Toupin [13] and Mindlin and Tiersten [8] showed that

$$\nabla_t S_{kl}^{(d)} = 2\eta\, e_{lmn}\partial_k\omega_{mn} + 2\eta'\, e_{kmn}\partial_l\omega_{mn} \tag{1.10}$$

with $\eta > 0$ and $-\eta < \eta' < \eta$. The constant η is called the bending-twisting modulus, and η'/η indicates the ratio of the transverse curvature to the principal curvature. The expression (1.10) implies that the rate of change of $S^{(d)}$ is related to the gradient of the spin rate tensor. We shall see in a later section that the inclusion of (1.10) has the effect of regularizing the rotational component of the solution.

Similarly, the pressure term $p\delta_{ij}$ in (1.4) regularizes the dilational component of the solution. We assume the following constitutive relation for p:

$$d_t p = \zeta\, \partial_{kk}\partial_l v_l \qquad \zeta > 0, \tag{1.11}$$

which relates the rate of change of the dispersive pressure to the rate of dilational change of the material.

It is easy to verify that

$$\sqrt{\frac{\zeta}{G}}, \qquad \sqrt{\frac{\eta}{G}} \tag{1.12}$$

have units of length. These quantities are related to the internal length scale of the material, for instance the void size or the grain size.

1.2. Reduction of the equations. In this section we combine the constitutive relations and eliminate the couple stress and dispersive pressure terms from the governing equations.

Combining (1.6), (1.7), and (1.9), we have

$$V_{ij} = \left(C_{ijkl} + \frac{1}{h} \Psi_{ij} \Phi_{kl} \right) \nabla_t T^{(s)}_{kl}.$$

Since the fourth-order tensor C is invertible, the above relation can be rewritten (cf. Lemma 1.3 in [1])

$$\nabla_t T^{(s)}_{ij} = \left(E_{ijkl} - \frac{1}{H} E_{ijmn} \Psi_{mn} \Phi_{rs} E_{rskl} \right) V_{kl}, \tag{1.13}$$

where E is given in (1.8) and H is defined as

$$H = h + \Phi_{ij} E_{ijkl} \Psi_{kl},$$

which is restricted to be strictly positive to exclude locking materials.

Multiplying (1.3) by e_{ijl} and using the identity

$$e_{ijl} e_{lmn} = \delta_{im} \delta_{jn} - \delta_{in} \delta_{jm},$$

we obtain

$$T^{(a)}_{ij} = \frac{1}{2} e_{ijl} \partial_k S_{kl} = \frac{1}{2} e_{ijl} \partial_k S^{(d)}_{kl} + \frac{1}{2n} e_{ijl} \partial_l S_{kk}, \tag{1.14}$$

where n is the dimension of space variables. Differentiating (1.14) with respect to t and using (1.10), we obtain

$$\nabla_t T^{(a)}_{ij} = 2\eta \, \partial_{kk} \omega_{ij} + \frac{1}{2n} e_{ijl} d_t (\partial_l S_{kk}). \tag{1.15}$$

Note that, if we only work on two-dimensional models, then (1.15) will reduce to

$$\nabla_t T^{(a)}_{12} = 2\eta \, \partial_{kk} \omega_{12}. \tag{1.16}$$

For easy reference, we rewrite the reduced system as follows:

$$\begin{aligned}
&d_t \rho + \rho \partial_j v_j = 0, \\
&\rho d_t v_j + \partial_i T_{ij} = 0, \\
&\nabla_t T_{ij} = \left(E_{ijkl} - \frac{\chi}{H} E_{ijmn} \Psi_{mn} \Phi_{rs} E_{rskl} \right) V_{kl} \\
&\qquad\qquad + \zeta \, \partial_{kk} \partial_l v_l \delta_{ij} + 2\eta \, \partial_{kk} \omega_{ij} + \frac{1}{2n} e_{ijl} d_t (\partial_l S_{kk}), \\
&\gamma_t = \frac{\chi}{h} \left(\Phi_{ij} \nabla_t T_{ij} \right)_+ ,
\end{aligned} \tag{1.17}$$

where χ is a characteristic function, which is zero when the material deforms elastically and is equal to one when the material begins to yield, and

$$a_+ = \begin{cases} a & \text{if } a > 0, \\ 0 & \text{otherwise.} \end{cases}$$

In (1.17), we include a new unknown, the total plastic shearing strain γ defined by

$$\gamma_t = \left|\operatorname{dev} V^{(p)}\right|.$$

The parameters h, μ, and β are assumed to be functions of γ.

In the isotropic hardening model, for instance, the yield condition is written as

$$\left|\left(T^{(s)}\right)^{(d)}\right| \leq \frac{1}{n} \operatorname{tr}\left(T^{(s)}\right) f(\gamma),$$

where $f(\gamma)$ is shown in Fig. 1.1 The functions μ and h are found as

$$\mu = f(\gamma), \qquad h = \frac{2}{n} \operatorname{tr}(T) f'(\gamma).$$

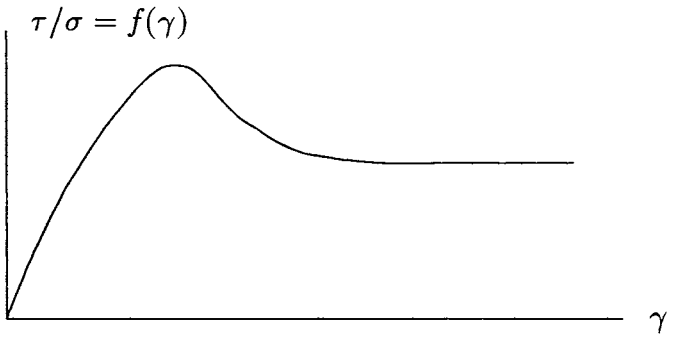

FIG. 1.1. *The ratio of shear stress to mean stress as a function of the total shear strain* γ.

Note that the third equation in (1.17) includes S_{kk}, whereas there is no additional equation that corresponds to it. Therefore, the trace of the couple stress as well as the antisymmetric part of T are left indeterminate except for two-dimensional models in which case this term is absent (cf. (1.16)).

Differentiating the second equation in (1.17) and using the third, we obtain

$$d_t(\rho d_t v_j) = \partial_i(B_{ijkl}\partial_l v_k) - \eta \partial_i \partial_{kk}(\partial_i v_j - \partial_j v_i) - \zeta \partial_j \partial_{kk} \partial_l v_l, \tag{1.18}$$

where

$$B_{ijkl} = E_{ijkl} + J_{ijkl} - \frac{\chi}{H} E_{ijmn} \Psi_{mn} \Phi_{rs} E_{rskl},$$

in which J_{ijkl} comes from the Jaumann derivative

$$J_{ijkl} = -\frac{1}{2}\left(\delta_{ik}T_{jl} - \delta_{il}T_{jk} + \delta_{jk}T_{il} - \delta_{jl}T_{ik}\right).$$

We see that terms containing η' and S_{kk} disappear in the equation of motion (1.18) independent of the number of dimensions of the model.

2. Review of previous work. Without the perturbation terms due to the microstructural parts of the model, the equation of motion (1.18) becomes

$$d_t(\rho d_t v_j) = \partial_i(B_{ijkl}\partial_l v_k), \tag{2.1}$$

which has been studied extensively [1], [2], [4], [6], [7], [10], [11]. If the body under consideration is in the elastic regime everywhere, then the equations of motion reduce to the equations of elastodynamics that are hyperbolic. The equation may still remain hyperbolic even though some of the regions of the body may have moved into the plastic regime. However, the initial value problem will become ill posed if within some region the equations lose their hyperbolicity. We therefore identify ill-posedness by linearizing the equation of motion about some nominal state and by looking for conditions under which the equation of motion changes type.

These conditions can be determined by expressing the perturbations v to the nominal strain rate $v^{(0)}$ in the following traveling wave form:

$$v_j = \hat{v}_j e^{i(x\cdot\xi - c(\xi)t)}. \tag{2.2}$$

Substituting (2.2) into (2.1) reduces the problem to the one of studying the eigenvalue structure of the following acoustic tensor:

$$A(\xi, h) = \frac{1}{\rho^{(0)}} \left(\xi_i B_{ijkl}\left(h, T^{(0)}, v^{(0)}\right) \xi_l\right), \tag{2.3}$$

where $\rho^{(0)}, T^{(0)}$, and $v^{(0)}$ are the nominal state variables and ξ is a unit vector indicating the direction of motion of the plane wave. The eigenvalues of (2.3) are the square of the wave speeds and the original equations are hyperbolic if and only if all eigenvalues of (2.3) are nonnegative.

There are two physical mechanisms that could cause the equations to become ill posed. Both modes of ill-posedness are direction-dependent, i.e., ill-posedness is initiated preferentially in well-defined traveling directions. The first mode of ill-posedness, called shear band ill-posedness, corresponds to the case in which the smallest eigenvalues of (2.3) become zero and then negative [7], [10], [11]. In this case stationary discontinuities (i.e., with zero velocities) could occur and shear bands are formed. Our task is to determine the value of the parameter h and in what direction ξ the smallest eigenvalue of (2.3) first becomes negative. The critical value h_s (the subscript s is used for "shear band" ill-posedness) of the hardening modulus can be expressed in the form:

$$h_s = \max\left\{h : \min_{|\xi|=1} \det A(\xi, h) < 0\right\},$$

where $\det A$ is the determinant of A and the direction ξ is determined. Hence, shear bands could be formed when $h < h_s$.

The second mode of ill-posedness, called flutter ill-posedness, corresponds to the case in which the two eigenvalues of (2.3) become equal and then complex with a nonzero real part [1], [2], [4], [6]. In this case, we could have moving discontinuities. It is believed that this ill-posedness is related to the slip-stick motion often observed inside a container such as a hopper. The value h and direction ξ for which this ill-posedness occurs can be determined by

$$\min_{|\xi|=1} \operatorname{disc} A(\xi, h) < 0 \quad \text{for some h},$$

where $\operatorname{disc} A$ is the discriminant of the characteristic polynomial of A.

We state the results [1] here for the two-dimensional case. For convenience, we let $\xi_1 = \cos\theta$ and $\xi_2 = \sin\theta$, where θ is the angle between the directions of the traveling wave and the major principal stress.

PROPOSITION 2.1. *The minimal value of the determinant, which is achieved at*

$$\cos 2\theta = -\frac{1}{2}(\mu + \beta),$$

will be negative for

$$h < h_s = \frac{G}{2(1-2\nu)}(\mu - \beta)^2.$$

PROPOSITION 2.2. *Generically, the minimal value of the discriminant, which is achieved near*

$$\theta = \frac{\pi}{2},$$

will be negative in a neighborhood of

$$h_f = 4G(\mu + \beta - 2\nu).$$

(here we use the subscript f for "flutter" ill-posedness).

For the three-dimensional case, the results are more complicated, especially for flutter ill-posedness. The interested reader can consult references [2], [6], [10].

In the two-dimensional case, when every point of the body falls outside the instability regime, i.e., when $h < h_s$ and h is also far away from h_f, the system

$$\rho\partial_t v_j + \partial_i T_{ij} = 0, \qquad \partial_t T_{ij} + B_{ijkl}\partial_l v_k = 0 \tag{2.4}$$

is strictly hyperbolic (i.e., has five distinct real eigenvalues). By using the theory of pseudodifferential operators [12], a global energy inequality can be obtained. Note that the system (2.4) is not symmetric and, in the proof, a direction-dependent symmetrizer is used (see Appendix A).

When the equations become ill posed, the amplitude of the plane wave solution will grow uncontrollably in some direction and the energy inequality will no longer hold. However, under the influence of microstructure, which is represented by terms involving fourth-order gradients of the solution multiplied by small parameters (1.18), rapidly growing components characteristic of ill-posedness could be either dispersed or dissipated. As a result of these microstructural singular perturbation terms, the regions of ill-posedness are replaced by well-defined internal damage layers that are formed in a stable fashion. In subsequent sections we analyze the effect of microstructure on the formation of these discontinuities.

3. Effect of microstructure.

3.1. Linear analysis. We restrict ourselves to two-dimensional models and carry out the linear analysis described above to see how the inclusion of microstructure affects the behavior of eigenvalues of the acoustic tensor.

Freezing the coefficients in (1.18) and substituting the exponential solution (2.2), we obtain the following equations:

$$\rho^{(0)}(c - v_k^{(0)}\xi_k)^2\hat{v}_j = \xi_i B_{ijkl}\xi_l\hat{v}_k + \eta(|\xi|^4\hat{v}_j - |\xi|^2\xi_l\xi_j\hat{v}_l) + \zeta|\xi|^2\xi_j\xi_l\hat{v}_l,$$

where $|\xi|^2 = \xi_1^2 + \xi_2^2$. Writing the above in matrix form, we have

$$\begin{pmatrix} \xi_i B_{i11l}\xi_l + |\xi|^2(\eta\xi_2^2 + \zeta\xi_1^2) & \xi_i B_{i12l}\xi_l + (\zeta - \eta)|\xi|^2\xi_1\xi_2 \\ \xi_i B_{i21l}\xi_l + (\zeta - \eta)|\xi|^2\xi_1\xi_2 & \xi_i B_{i22l}\xi_l + |\xi|^2(\eta\xi_1^2 + \zeta\xi_2^2) \end{pmatrix} \begin{pmatrix} \hat{v}_1 \\ \hat{v}_2 \end{pmatrix}$$
$$= \rho^{(0)}\left(c - v_k^{(0)}\xi_k\right)^2 \begin{pmatrix} \hat{v}_1 \\ \hat{v}_2 \end{pmatrix}.$$

We do not assume $|\xi| = 1$ here, since the matrix in the above is not homogeneous in ξ. Note that, compared with ∂_t, the extra term $v_k^{(0)}\xi_k$ in d_t only causes a small shift ($|v^{(0)}| \sim 5 \times 10^{-5}$ cm/sec) of the eigenvalues. Later, we shall use ∂_t instead of d_t.

If we denote the above matrix by

$$\begin{pmatrix} A_{11} & A_{12} \\ A_{21} & A_{22} \end{pmatrix},$$

then its eigenvalues are given by

$$\lambda_{1,2} = \frac{1}{2}\left\{\mathrm{tr}(A) \pm \sqrt{\mathrm{disc}(A)}\right\}. \tag{3.1}$$

The smaller eigenvalue can be written as

$$\lambda_2 = \frac{2 \cdot \det(A)}{\mathrm{tr}(A) + \sqrt{\mathrm{disc}(A)}}. \tag{3.2}$$

Note that $\lambda = \rho^{(0)}\left(c - v_k^{(0)}\xi_k\right)^2$. To guarantee well-posedness, we require both eigenvalues λ_1, λ_2 to be real and nonnegative. When $\zeta + \eta \geq 0$,

$$\mathrm{tr}(A) = \xi_i B_{i11l}\xi_l + \xi_i B_{i22l}\xi_l + (\zeta + \eta)|\xi|^4$$

will be positive. Hence, it follows from (3.1) and (3.2) that the equations are well posed if and only if both $\det(A)$ and $\mathrm{disc}(A)$ are positive.

(i) *Shear band ill-posedness.* It is easy to check that

$$\begin{aligned}\det(A) = {} & \left[(\xi_i B_{i11l}\xi_l)(\xi_p B_{p22q}\xi_q) - (\xi_i B_{i12l}\xi_l)(\xi_p B_{p21q}\xi_q)\right] \\ & + |\xi|^2\Big\{\zeta\eta|\xi|^6 - (\zeta - \eta)\xi_1\xi_2(\xi_i B_{i12l}\xi_l + \xi_i B_{i21l}\xi_l) \\ & \qquad + (\eta\xi_2^2 + \zeta\xi_1^2)(\xi_i B_{i22l}\xi_l) + (\eta\xi_1^2 + \zeta\xi_2^2)(\xi_i B_{i11l}\xi_l)\Big\}.\end{aligned}$$

The first term is the determinant without perturbation, which will be negative for the values of (ξ, h) given in Proposition 2.1. But when $\zeta\eta > 0$, it follows from (3.2) that the small eigenvalue will be positive for large wave numbers ξ. So shear band ill-posedness does not occur when the microstructure terms are present.

(ii) *Flutter ill-posedness.* Now we calculate the discriminant

$$\begin{aligned}\mathrm{disc}(A) = {} & \left[(\xi_i B_{i11l}\xi_l - \xi_i B_{i22l}\xi_l)^2 + 4(\xi_i B_{i12l}\xi_l)(\xi_p B_{p21q}\xi_q)\right] \\ & + |\xi|^2\Big\{(\zeta - \eta)^2|\xi|^6 + 4(\zeta - \eta)\xi_1\xi_2(\xi_i B_{i12l}\xi_l + \xi_i B_{i21l}\xi_l) \\ & \qquad + 2(\xi_i B_{i11l}\xi_l - \xi_i B_{i22l}\xi_l)(\zeta - \eta)(\xi_1^2 - \xi_2^2)\Big\}.\end{aligned}$$

The first term is the discriminant without perturbation, which could be negative for some values of (ξ, h) (cf. Proposition 2.2). But when $\zeta \neq \eta$ (the generic case), the

discriminant will be positive for large wave numbers ξ. So flutter ill-posedness does not occur when the microstructure terms are present and when $\zeta \neq \eta$.

In the case $\zeta = \eta$, we have

$$\operatorname{disc}(A) = \operatorname{disc}(A^{(0)}) < 0,$$

when h is near h_f and θ is near $\pi/2$, and where $\operatorname{disc}(A^{(0)})$ is the discriminant without perturbation. However, we claim that the growth rate of the eigenvalue is still finite. To prove this we need to study the real part of the square roots of $\lambda_{1,2}$

$$\operatorname{Re}\left(\sqrt{\lambda_{1,2}}\right) = \frac{1}{\sqrt{2}}\left(\operatorname{tr}^2(A) - \operatorname{disc}(A)\right)^{1/4} \sin\frac{\alpha}{2},$$

where $\alpha = \arg\left(\operatorname{tr}(A) + i\sqrt{-\operatorname{disc}(A)}\right)$. It is easy to check that, as $\xi \to \infty$,

$$\operatorname{tr}(A) \sim 2\eta|\xi|^4, \qquad \operatorname{disc}(A) \sim O(|\xi|^4).$$

It follows that, as $\xi \to \infty$,

$$\sin\frac{\alpha}{2} = \left\{\frac{-\operatorname{disc}(A)}{2\sqrt{\operatorname{tr}^2(A) - \operatorname{disc}(A)}\left(\sqrt{\operatorname{tr}^2(A) - \operatorname{disc}(A)} + \operatorname{tr}(A)\right)}\right\}^{1/2} \sim O(|\xi|^{-2}).$$

Therefore as $\xi \to \infty$,

$$\operatorname{Re}\left(\sqrt{\lambda_{1,2}}\right) \sim \sqrt{\eta}|\xi|^2 O(|\xi|^{-2})$$

from which it follows that $\operatorname{Re}\left(\sqrt{\lambda_{1,2}}\right)$ is bounded.

Dispersion provides another interpretation of the way the microstructure terms can work to inhibit the onset of ill-posedness. Since (3.1) involves terms in ξ having different degrees, the expression (3.1) forms a dispersion relation when the governing equation is still hyperbolic (i.e., when both $\det(A)$ and $\operatorname{disc}(A)$ are positive). Waves with different wave numbers ξ will move at different speeds and the phase and group speeds will be different. Specifically, the phase speed

$$\pm\frac{\sqrt{\lambda_i(\xi)}}{|\xi|} \qquad \text{i=1,2}$$

will tend to ∞ as the wave number ξ tends to ∞. Therefore when the equations approach ill-posedness, the concentrated discontinuities (associated with the high frequency components $\xi \to \infty$) are dispersed extremely rapidly thereby inhibiting ill-posedness. In the absence of the microstructure terms, (3.1) is quadratic in ξ, which implies that the medium is not dispersive in the limit $\xi \to \infty$ so that the concentrated discontinuities associated with ill-posedness can possibly be formed.

Locally, the equations of motion in the dilational and in the rotational directions can be expressed by

$$\rho^{(0)}\partial_{tt}(\partial_j v_j) = \partial_{ij}(B_{ijkl}\partial_l v_k) - \zeta\partial_{jj}\partial_{kk}\partial_l v_l,$$
$$\rho^{(0)}\partial_{tt}(e_{pqj}\partial_q v_j) = e_{pqj}\partial_{qi}(B_{ijkl}\partial_l v_k) - \eta\partial_{ii}\partial_{kk}(e_{pqj}\partial_q v_j),$$

respectively. Clearly, these expressions show us that Cosserat theory only affects the behavior of solutions in the rotational direction, while the dispersive pressure term only affects the behavior of solution in the dilational direction. However, when the original equations reach ill-posedness, the eigendirections are not necessarily in longitudinal and transverse directions. Therefore, generally both types of microstructure must be present to regularize the behavior of solutions.

Incidentally, if we could add a diffusion term to the momentum conservation equation, we would obtain the following equations:

$$\rho\partial_t v_j + \partial_i T_{ij} = 2\rho\epsilon\partial_{kk}v_j, \qquad \partial_t T_{ij} = -B_{ijkl}\partial_l v_k + \rho\epsilon^2\partial_i\partial_{kk}v_j, \tag{3.3}$$

then we can obtain a dissipative effect on the behavior of the solution. In fact, combining these two equations, we have

$$\rho\partial_{tt}v_j - \partial_i(B_{ijkl}\partial_l v_k) - 2\rho\epsilon\partial_{kk}\partial_t v_j + \rho\epsilon^2\partial_{ii}\partial_{kk}v_j = 0.$$

Equivalently,

$$\rho(\partial_t - \epsilon\partial_{kk})^2 v_l = \partial_i(B_{ijkl}\partial_l v_k).$$

The corresponding eigenvalue problem has the form

$$(c + i\epsilon|\xi|^2)^2 v_j = \frac{1}{\rho^{(0)}}\xi_i B_{ijkl}\xi_l v_k,$$

which yields

$$c = -i\epsilon|\xi|^2 \pm \sqrt{\lambda_j},$$

where λ_j $(j = 1, 2, 3)$ are eigenvalues of

$$\frac{1}{\rho^{(0)}}\xi_i B_{ijkl}\xi_l.$$

The following type of solution

$$e^{i(x\cdot\xi - ct)}$$

will decay exponentially as $\xi \to \infty$. Note that the extra term in the second equation of (3.3) can be obtained by letting $\zeta = \eta$ in the previous microstructure formulation.

3.2. Integral estimate. When we include the microstructure terms into the model, the L^2-norm of the gradient of velocity can be controlled under appropriate boundary conditions. The analysis that follows provides another demonstration of the fact that the microstructure regularizes the behavior of the solution. Instead of giving a rigorous mathematical proof, we sketch the calculation to show how the L^2-norm of the gradient can be bounded.

Multiplying (1.18) by $\partial_t v_j$ and then integrating over $(t_0, t) \times \Omega$, we have

$$\begin{aligned}\int_{t_0}^{t}\int_\Omega \partial_t v_j \partial_t(\rho\partial_t v_j)dxd\tau - \int_{t_0}^{t}\int_\Omega \partial_i(B_{ijkl}\partial_l v_k)\partial_t v_j dxd\tau \\ + \int_{t_0}^{t}\int_\Omega \eta\partial_i\partial_{kk}(\partial_i v_j - \partial_j v_i)\partial_t v_j dxd\tau \\ + \int_{t_0}^{t}\int_\Omega \zeta\partial_j\partial_{kk}\partial_l v_l \partial_t v_j dxd\tau = 0.\end{aligned} \tag{3.4}$$

It is easy to check that

$$\int_{t_0}^{t}\int_{\Omega}\partial_t v_j \partial_t(\rho\partial_t v_j)dxd\tau = \int_{t_0}^{t}\int_{\Omega}\left(\partial_t\left(\frac{\rho}{2}\partial_t v_j\partial_t v_j\right) - \frac{\partial_t\rho}{2}\partial_t v_j\partial_t v_j\right)dxd\tau. \tag{3.5}$$

Regrouping the third and fourth terms in (3.4) and then integrating by parts twice, we have (assuming that $\eta \geq \zeta$)

(3.6)

$$\begin{aligned}
&(\eta-\zeta)\int_{t_0}^{t}\int_{\Omega}\partial_i\partial_{kk}(\partial_i v_j - \partial_j v_i)\partial_t v_j dxd\tau + \zeta\int_{t_0}^{t}\int_{\Omega}\partial_i\partial_{kk}\partial_i v_j\partial_t v_j dxd\tau\\
&= (\eta-\zeta)\int_{t_0}^{t}\int_{\partial\Omega}\partial_{kk}(\partial_i v_j - \partial_j v_i)n_i\partial_t v_j dsd\tau + \zeta\int_{t_0}^{t}\int_{\partial\Omega}\partial_{kk}\partial_i v_j n_i\partial_t v_j dsd\tau\\
&\quad - (\eta-\zeta)\int_{t_0}^{t}\int_{\partial\Omega}n_k\partial_k(\partial_i v_j - \partial_j v_i)\partial_t(\partial_i v_j)dsd\tau - \zeta\int_{t_0}^{t}\int_{\partial\Omega}n_k\partial_{ki}v_j\partial_t(\partial_i v_j)dsd\tau\\
&\quad + (\eta-\zeta)\int_{t_0}^{t}\int_{\Omega}\partial_k(\partial_i v_j - \partial_j v_i)\partial_t(\partial_{ki}v_j)dxd\tau + \zeta\int_{t_0}^{t}\int_{\Omega}\partial_k\partial_i v_j\partial_t(\partial_{ki}v_j)dxd\tau,
\end{aligned}$$

where $\partial\Omega$ is the boundary of Ω and n the unit outwards vector normal to Ω. Substitution of (3.5) and (3.6) in (3.4) gives

(3.7)

$$\begin{aligned}
&\left(\int_{\Omega}\left(\rho\partial_t v_j\partial_t v_j + (\eta-\zeta)\partial_k(\partial_i v_j - \partial_j v_i)\partial_k(\partial_i v_j - \partial_j v_i) + \zeta\partial_{ki}v_j\partial_{ki}v_j\right)dx\right)(t)\\
&\quad + \int_{t_0}^{t}\int_{\Omega}\partial_t\rho\partial_t v_j\partial_t v_j dxd\tau - 2\int_{t_0}^{t}\int_{\Omega}\partial_i(B_{ijkl}\partial_l v_k)\partial_t v_j dxd\tau\\
&= \left(\int_{\Omega}\left(\rho\partial_t v_j\partial_t v_j + (\eta-\zeta)\partial_k(\partial_i v_j - \partial_j v_i)\partial_k(\partial_i v_j - \partial_j v_i) + \zeta\partial_{ki}v_j\partial_{ki}v_j\right)dx\right)(t_0)\\
&\quad + (\text{integrals along boundary}).
\end{aligned}$$

Under proper boundary and initial conditions, the integral on the right-hand side of (3.7) is finite. The equality (3.7) implies that

(3.8)

$$\begin{aligned}
&\left(\int_{\Omega}\frac{\rho}{2}\partial_t v_j\partial_t v_j dx + \int_{\Omega}\frac{\zeta}{2}\partial_k\partial_i v_j\partial_k\partial_i v_j dx\right)(t)\\
&\leq \int_{t_0}^{t}\int_{\Omega}\left|\frac{1}{2}\partial_t\rho\partial_t v_j\partial_t v_j\right|dxd\tau + \int_{t_0}^{t}\int_{\Omega}\left|\partial_i(B_{ijkl}\partial_l v_k)\partial_t v_j\right|dxd\tau + C,
\end{aligned}$$

where C is a constant.

The interpolation inequality for Hilbert space $H^2(\Omega)$ gives

$$\left(\int_{\Omega}\sum_{l}|\partial_l v_k|^2 dx\right)(t) \leq C\left(\int_{\Omega}|v_k|^2 dx + \int_{\Omega}\sum_{ij}|\partial_{ij}v_k|^2\right)(t). \tag{3.9}$$

It is also easy to check that

$$\left(\int_{\Omega}|v_k|^2 dx\right)(t) \leq \left(\int_{\Omega}|v_k|^2 dx\right)(t_0) + \int_{t_0}^{t}\int_{\Omega}|\partial_t v_j|^2 d\tau dx. \tag{3.10}$$

It follows from (3.9), (3.10), and the Hölder inequality that

$$\int_{t_0}^{t}\int_{\Omega}|\partial_i(B_{ijkl}\partial_l v_k)\partial_t v_j|dxd\tau \leq C\left\{\left(\int_{\Omega}\sum_k |v_k|^2 dx\right)(t_0)+\int_{t_0}^{t}\int_{\Omega}\left(\sum_{ij}|\partial_{ij}v_k|^2+\sum_j|\partial_t v_j|^2\right)dxdt\right\}.$$

Now, (3.8) becomes

$$\left(\int_{\Omega}\rho\partial_t v_j\partial_t v_j dx+\int_{\Omega}\zeta\partial_{ki}v_j\partial_{ki}v_j dx\right) \leq C\int_{t_0}^{t}\int_{\Omega}\left(\rho\sum_j|\partial_t v_j|^2+\zeta\sum_{kij}|\partial_{ki}v_j|^2\right)dxd\tau+C'.$$

By Gronwall's inequality,

$$\left(\int_{\Omega}\rho(\partial_t v_j\partial_t v_j)dx+\int_{\Omega}\zeta\left(\partial_{ki}v_j\partial_{ki}v_j\right)dx\right)(t)\leq C.$$

Applying (3.9) and (3.10) again, we obtain

$$\int_{\Omega}\sum_j|\partial_t v_j|^2dx+\int_{\Omega}\sum_{lk}|\partial_l v_k|^2dx+\int_{\Omega}\sum_{ijk}|\partial_{ij}v_k|^2dx\leq C.$$

From the calculation, we can see that both ζ and η should be positive to control the L^2-norm of the gradient of velocity. This also corresponds to the fact that the specific internal energy regarded as a function of the strain rate, the gradient of rotation rate, and the gradient of dilation rate should be positive definite with respect to its variables. Therefore as a result of deformation, the energy should be stored rather than released. In general, the positive definiteness of the energy functional guarantees uniqueness of solutions.

4. Singular perturbations. The terms representing the microstructure involve the highest-order derivatives in the governing equations and the coefficients of these terms are small compared to the shear modulus (cf. 1.12). Therefore the governing equations (1.18) form a singular perturbation problem. When the equations reach the critical state at some interior points, inhomogeneity in the solution will grow in the directions predicted by the previous work in §2. Deformation will be localized in these regions and as a result the higher-order gradients will play a dominant role.

In this section we show that by introducing local variables it is possible to reduce the governing equations to time-independent singular Schrödinger equations in which the potentials have two turning points. The turning points are associated with the boundaries of the region of ill-posedness and by making use of classical WKB theory and leading-order matched asymptotics it is possible to relate the thickness of localization region and the internal length scale (1.12) of the material.

4.1. Shear band ill-posedness. For simplicity, we assume that $\zeta = \eta$, in which case the equation of motion becomes

$$\partial_t(\rho\partial_t v_j) = \partial_i(B_{ijkl}\partial_l v_k) - \eta\partial_{ii}\partial_{kk}v_j. \tag{4.1}$$

Without loss of generality, we also assume that the equations reach the onset of shear band ill-posedness in a neighborhood of $x = 0$, and that the direction of the major principal stress is parallel to the x_1-direction near $x = 0$. In terms of Proposition 2.1, the inhomogeneity will grow in the direction $\xi = (\cos\theta_0, \sin\theta_0)$, where $\cos(2\theta_0) = -\frac{1}{2}(\mu + \beta)$.

In a neighborhood of $x = 0$, we are looking for solutions of form

$$v(x,t) = u(z), \qquad z = x_1\xi_1 + x_2\xi_2.$$

This form of trial solution is motivated by the fact that we are looking for a traveling wave solution with a zero wave speed to capture the stationary shear band instability. Substituting the trial solution into (4.1), we obtain

$$\eta\begin{pmatrix}u_1\\u_2\end{pmatrix}^{(4)} - \begin{pmatrix}\xi_i B_{i11l}\xi_l & \xi_i B_{i12l}\xi_l\\ \xi_i B_{i21l}\xi_l & \xi_i B_{i22l}\xi_l\end{pmatrix}\begin{pmatrix}u_1\\u_1\end{pmatrix}'' - \begin{pmatrix}\partial_i B_{i11l}\xi_l & \partial_i B_{i12l}\xi_l\\ \partial_i B_{i21l}\xi_l & \partial_i B_{i22l}\xi_l\end{pmatrix}\begin{pmatrix}u_1\\u_1\end{pmatrix}' = 0. \tag{4.2}$$

Let (a,b) be the unit left eigenvector of $(\xi_i B_{ijkl}\xi_l)$ corresponding to the small eigenvalue and define the quantity

$$U = a\,u_1 + b\,u_2,$$

which is the Riemann invariant corresponding to the smaller eigenvalue. Multiplying (4.2) on the left by (a, b), we obtain

$$\eta U^{(4)} - \lambda(z)U'' + O(\text{other terms}) = 0, \tag{4.3}$$

where other terms $= O(U', \eta U^{(3)})$, i.e., lower than second-order derivatives and lower than fourth-order derivatives multiplied by the small parameter η. Assume that $\lambda(z) < 0$ for $|z| < \delta$, $\lambda(z) > 0$ for $|z| > \delta$, and that the turning points $|z| = \delta$ identify the boundary of the region of shear band ill-posedness. In terms of Proposition 2.1,

$$h = h_s \quad \text{at } |z| = \delta.$$

Equation (4.3) has two turning points $z = \pm\delta$. So from classical WKB theory [5] asymptotic matching at the leading-order requires

$$\frac{1}{\sqrt{\eta}}\int_{-\delta}^{\delta}\sqrt{-\lambda(z)}\,dz = \left(n + \frac{1}{2}\right)\pi + O\left(\sqrt{\frac{\eta}{G}}\right).$$

Let $n = 0$, then the expression

$$\frac{1}{\sqrt{\eta}}\int_{-\delta}^{\delta}\sqrt{-\lambda(z)}\,dz = \frac{\pi}{2} + O\left(\sqrt{\frac{\eta}{G}}\right)$$

relates the thickness of shear band 2δ to the internal length scale $\sqrt{\frac{\eta}{G}}$ of the material.

4.2. Flutter ill-posedness. We know from Proposition 2.2 that there is a neighborhood of h_f such that the minimal value of the discriminant is negative. Therefore, there exists a lower limit $h_f^{(l)}$ and an upper limit $h_f^{(u)}$, such that when $h \in \left(h_f^{(l)}, h_f^{(u)}\right)$ the governing equations exhibit flutter ill-posedness. Following the analysis in the previous subsection, we assume that the equations reach flutter ill-posedness around $x = 0$, and that the direction of the major principal stress is parallel to the x_1-direction. In terms of Proposition 2.2, the inhomogeneity will grow in the direction $\xi = (\cos\theta_0, \sin\theta_0)$ where $\theta_0 = \pi/2$. From the following WKB analysis, we see that if $\eta \neq \zeta$ then the solutions that decay at both ends $z \to \pm\infty$ can be obtained through an asymptotic matching process and the match conditions reveal the relation between the thickness of boundary layer and parameters η and ζ. The nongeneric case $\eta = \zeta$ is treated in Appendix B.

In a neighborhood of $x = 0$, we are looking for solutions of form

$$v(x,t) = u(z), \qquad z = x_1\xi_1 + x_2\xi_2 - c_0 t,$$

where c_0 is given by

$$\rho^{(0)} c_0^2 = \frac{1}{2}(\xi_i B_{i11l}\xi_l + \xi_i B_{i22l}\xi_l).$$

Substituting this trial solution into (4.1), we obtain

(4.4)
$$\begin{pmatrix}\eta u_1\\ \zeta u_2\end{pmatrix}^{(4)} - \begin{pmatrix} \dfrac{(\xi_i B_{i11l}\xi_l - \xi_i B_{i22l}\xi_l)}{2} & \xi_i B_{i12l}\xi_l \\ \xi_i B_{i21l}\xi_l & -\dfrac{(\xi_i B_{i11l}\xi_l - \xi_i B_{i22l}\xi_l)}{2}\end{pmatrix}\begin{pmatrix}u_1\\ u_2\end{pmatrix}'' + \ldots = 0.$$

Let $a_{11} = (\xi_i B_{i11l}\xi_l - \xi_i B_{i22l}\xi_l)/2$, $a_{12} = \xi_i B_{i12l}\xi_l$, and $a_{21} = \xi_i B_{i21l}\xi_l$. Since the discriminant $\mathrm{disc}(A)/4 = a_{11}^2 + a_{12}a_{21}$ is negative near $z = 0$, we assume that $a_{11}^2 + a_{12}a_{21} < 0$ for $|z| < \delta$ and $a_{11}^2 + a_{12}a_{21} > 0$ for $|z| > \delta$. The points $|z| = \delta$ identify the boundary of the region of flutter ill-posedness. In other words,

$$h = h_f^{(l)} \text{ or } h_f^{(u)} \quad \text{at } |z| = \delta.$$

Assume that $\eta = \epsilon^2/\hat{\eta}$ and $\zeta = \epsilon^2/\hat{\zeta}$, where $\hat{\eta} = O(1) = \hat{\zeta}$. The system (4.4) becomes

$$\epsilon^2\begin{pmatrix}u_1\\ u_2\end{pmatrix}^{(4)} = \begin{pmatrix} a_{11}\hat{\eta} & a_{12}\hat{\eta} \\ a_{21}\hat{\zeta} & -a_{11}\hat{\zeta}\end{pmatrix}\begin{pmatrix}u_1\\ u_2\end{pmatrix}'' + (\text{l.o.t.}) = 0.$$

The eigenvalues of the matrix in the above formula are

$$Q_{1,2} = a_{11}\frac{\hat{\eta} - \hat{\zeta}}{2} \pm \sqrt{a_{11}^2\left(\frac{\hat{\eta} + \hat{\zeta}}{2}\right)^2 + a_{12}a_{21}\hat{\eta}\hat{\zeta}}.$$

Note that since $h = h_f$ is the first value of h at which the onset of flutter ill-posedness occurs, $a_{11} = 0$ at $h = h_f$ and when $\hat{\eta} \neq \hat{\zeta}$,

$$(a_{11}^2 + a_{12}a_{21})\,\hat{\eta}\hat{\zeta} < a_{11}^2\left(\frac{\hat{\zeta} + \hat{\eta}}{2}\right)^2 + a_{12}a_{21}\hat{\eta}\hat{\zeta}.$$

There are, therefore, two points z_1 and z_2 that determine where the Q_i become complex. These points are such that $-\delta < z_1 < z_2 < \delta$ and

$$a_{11}^2\left(\frac{\hat{\zeta}+\hat{\eta}}{2}\right)^2 + a_{12}a_{21}\hat{\eta}\hat{\zeta} < 0 \quad \text{for } z \in (z_1, z_2),$$
$$a_{11}^2\left(\frac{\hat{\zeta}+\hat{\eta}}{2}\right)^2 + a_{12}a_{21}\hat{\eta}\hat{\zeta} > 0 \quad \text{for } z \notin [z_1, z_2].$$

We now perform a WKB analysis for the system

$$\epsilon^2\begin{pmatrix} u_1 \\ u_2 \end{pmatrix}'' = \begin{pmatrix} a_{11}\hat{\eta} & a_{12}\hat{\eta} \\ a_{21}\hat{\zeta} & a_{22}\hat{\zeta} \end{pmatrix}\begin{pmatrix} u_1 \\ u_2 \end{pmatrix}.$$

We are looking for solutions u_i $(i = 1, 2)$ that are linear combinations of four of the independent solutions of

$$\epsilon^2 w'' = Q_1(z)w, \qquad \epsilon^2 \hat{w}'' = Q_2(z)\hat{w}.$$

By the WKB method, we know that when $Q(\lambda) \neq 0$, the leading-order parts of the solution are

$$w \sim |Q|^{-1/4}\exp\left(\frac{1}{\epsilon}\int_a^z \omega_i |Q|^{1/2} ds\right),$$

where ω_i is one of the square roots of $Q/|Q|$.

Without loss of generality, we assume that $\bar{\eta} > \bar{\zeta}$. Note that a_{11} could be negative or positive at $z = z_1$ or z_2. Here we only analyze one case, namely, the one in which

$$a_{11}(z_1) < 0 \quad \text{and} \quad a_{11}(z_2) > 0$$

(while other cases follow analogously). Under these assumptions, the behavior of Q_i is demonstrated in Table 4.1.

First, we start from region IV $= (z_2, +\infty)$. It follows from the decay requirement that

$$V_{\text{IV}} \sim C|Q_1|^{-1/4}\exp\left(-\frac{1}{\epsilon}\int_{z_2}^z |Q_1|^{1/2} ds\right).$$

Near the point $B = \{z_2\}, Q_1 \sim a + b(z - z_2) + \sqrt{c(z - z_2)}$, where $a,\ c > 0$. Hence

$$V_B \sim Ca^{-1/4}\exp\left(-\frac{1}{\epsilon}a(z - z_2)\right).$$

In the region III $= (z_1, z_2)$, $|Q_1| = |Q_2|$ and the square roots of $|Q_i|$ $(i = 1, 2)$ are denoted by ω, $\bar{\omega}$, $-\omega$, $-\bar{\omega}$, where $\text{Re}(\omega) > 0$ and $\text{Im}(\omega) > 0$ and $\bar{\omega}$ is the conjugate of ω. By asymptotic matching with V_B near $z = z_2$, we have

$$V_{\text{III}}^{(r)} \sim \frac{C}{2}|Q|^{-1/4}\left[\exp\left(\frac{1}{\epsilon}\int_z^{z_2} \omega|Q|^{1/2} ds\right) + \exp\left(\frac{1}{\epsilon}\int_z^{z_2} \bar{\omega}|Q|^{1/2} ds\right)\right],$$

where superscript (r) indicates that the solution has been matched from the right.

TABLE 4.1

	I	II	III	IV	
	$(-\infty, -\delta)$	$(-\delta, z_1)$	(z_1, z_2)	(z_2, δ)	$(\delta, +\infty)$
Q_1	+	−	Complex		+
Q_2	−		Complex	+	−

Second, we start from the region $\mathrm{I} = (-\infty, -\delta)$. It follows from the decay requirement that

$$V_{\mathrm{I}} \sim D|Q_1|^{-1/4} \exp\left(-\frac{1}{\epsilon}\int_z^{-\delta} |Q_1|^{1/2} ds\right).$$

Using the formula given in [5, p. 513], we have in the region $\mathrm{II} = (-\delta, z_1)$,

$$V_{\mathrm{II}} \sim 2D|Q_1|^{-1/4} \sin\left(\frac{1}{\epsilon}\int_{-\delta}^{z} |Q_1|^{1/2} ds + \frac{\pi}{4}\right).$$

Near the point $A = \{z_1\}$, $Q_1 \sim -a_1 + b_1(z - z_1) + \sqrt{c_1(z_1 - z)}$, where $a_1,\ c_1 > 0$. Hence,

$$V_A \sim 2Da_1^{-1/4} \sin\left(\frac{1}{\epsilon}\int_{-\delta}^{z_1} |Q_1|^{1/2} ds + \frac{\pi}{4} - \frac{1}{\epsilon}\sqrt{a_1}(z_1 - z)\right).$$

By asymptotic matching with V_A near $z = z_1$, we have, in the region $\mathrm{III} = (z_1, z_2)$,

$$\begin{aligned}
V_{\mathrm{III}}^{(l)} \sim\ & \beta_1 |Q_1|^{-1/4} \left\{ \sin\left(\frac{1}{\epsilon}\int_{-\delta}^{z_1} |Q_1|^{1/2} ds + \frac{\pi}{4}\right) \right. \\
& \cdot \frac{1}{2}\left[\exp\left(\frac{1}{\epsilon}\int_{z_1}^{z} \omega |Q_1|^{1/2} ds\right) + \exp\left(\frac{1}{\epsilon}\int_{z_1}^{z} \bar{\omega} |Q_1|^{1/2} ds\right)\right] \\
& + \cos\left(\frac{1}{\epsilon}\int_{-\delta}^{z_1} |Q_1|^{1/2} ds + \frac{\pi}{4}\right) \\
& \left. \cdot \frac{1}{2i}\left[\exp\left(\frac{1}{\epsilon}\int_{z_1}^{z} \omega |Q_1|^{1/2} ds\right) - \exp\left(\frac{1}{\epsilon}\int_{z_1}^{z} \bar{\omega} |Q_1|^{1/2} ds\right)\right] \right\} \\
& + \beta_2 |Q_1|^{-1/4} \left\{ \sin\left(\frac{1}{\epsilon}\int_{-\delta}^{z_1} |Q_1|^{1/2} ds + \frac{\pi}{4}\right) \right. \\
& \cdot \frac{1}{2}\left[\exp\left(\frac{-1}{\epsilon}\int_{z_1}^{z} \omega |Q_1|^{1/2} ds\right) + \exp\left(\frac{-1}{\epsilon}\int_{z_1}^{z} \bar{\omega} |Q_1|^{1/2} ds\right)\right] \\
& - \cos\left(\frac{1}{\epsilon}\int_{-\delta}^{z_1} |Q_1|^{1/2} ds + \frac{\pi}{4}\right) \\
& \left. \cdot \frac{1}{2i}\left[\exp\left(\frac{-1}{\epsilon}\int_{z_1}^{z} \omega |Q_1|^{1/2} ds\right) - \exp\left(\frac{-1}{\epsilon}\int_{z_1}^{z} \bar{\omega} |Q_1|^{1/2} ds\right)\right] \right\},
\end{aligned}$$

where $\beta_1 + \beta_2 = 2D$ and superscript (l) indicates that the solution has been matched from the left. To compare $V_{\mathrm{III}}^{(l)}$ with $V_{\mathrm{III}}^{(r)}$ in the region III, we write them in appropriate form,

$$\begin{aligned}
V_{\mathrm{III}}^{(l)} \sim\ & \beta_1 |Q_1|^{-1/4} \exp\left(\frac{1}{\epsilon}\int_{z_1}^{z_2} \mathrm{Re}(\omega) |Q_1|^{1/2} ds\right) \exp\left(\frac{-1}{\epsilon}\int_{z}^{z_2} \mathrm{Re}(\omega) |Q_1|^{1/2} ds\right) \\
& \cdot \sin\left(\frac{1}{\epsilon}\int_{-\delta}^{z_1} |Q_1|^{1/2} ds + \frac{1}{\epsilon}\int_{z_1}^{z_2} \mathrm{Im}(\omega) |Q_1|^{1/2} ds + \frac{\pi}{4} - \frac{1}{\epsilon}\int_{z}^{z_2} \mathrm{Im}(\omega) |Q_1|^{1/2} ds\right) \\
& + \beta_2 |Q_1|^{-1/4} \exp\left(\frac{-1}{\epsilon}\int_{z_1}^{z_2} \mathrm{Re}(\omega) |Q_1|^{1/2} ds\right) \exp\left(\frac{1}{\epsilon}\int_{z}^{z_2} \mathrm{Re}(\omega) |Q_1|^{1/2} ds\right) \\
& \cdot \sin\left(\frac{1}{\epsilon}\int_{-\delta}^{z_1} |Q_1|^{1/2} ds + \frac{1}{\epsilon}\int_{z_1}^{z_2} \mathrm{Im}(\omega) |Q_1|^{1/2} ds + \frac{\pi}{4} - \frac{1}{\epsilon}\int_{z}^{z_2} \mathrm{Im}(\omega) |Q_1|^{1/2} ds\right), \\
V_{\mathrm{III}}^{(r)} \sim\ & C|Q_1|^{-1/4} \exp\left(\frac{1}{\epsilon}\int_{z}^{z_2} \mathrm{Re}(\omega) |Q_1|^{1/2} ds\right) \sin\left(\frac{\pi}{2} - \frac{1}{\epsilon}\int_{z}^{z_2} \mathrm{Im}(\omega) |Q_1|^{1/2} ds\right).
\end{aligned}$$

The identity $V_{\text{III}}^{(r)} \equiv V_{\text{III}}^{(l)}$ requires $\beta_1 = 0$, $\beta_2 = 2D$, and

$$\frac{1}{\epsilon}\int_{-\delta}^{z_1} |Q_1|^{1/2} ds + \frac{1}{\epsilon}\int_{z_1}^{z_2} \text{Im}(\omega)|Q_1|^{1/2} ds - \frac{\pi}{4} = n\pi + O\left(\frac{\epsilon}{\sqrt{G}}\right),$$
$$2D(-1)^n \exp\left(\frac{-1}{\epsilon}\int_{z_1}^{z_2} \text{Re}(\omega)|Q_1|^{1/2} ds\right) = C.$$

Choosing $n = 0$, we obtain

$$\frac{1}{\epsilon}\int_{-\delta}^{z_1} |Q_1|^{1/2} ds + \frac{1}{\epsilon}\int_{z_1}^{z_2} \text{Im}(\omega)|Q|^{1/2} ds = \frac{\pi}{4} + O\left(\frac{\epsilon}{\sqrt{G}}\right),$$

which relates the thickness of the region of "flutter" localization 2δ to the internal length scale $\epsilon/\sqrt{G}$ of the material.

In contrast, if $\hat{\eta} = \hat{\zeta}$, then $a = a_1 = 0$ and solutions that decay at both ends cannot be obtained. In fact, in this case, we need to analyze the following two turning point problem

$$\epsilon^4 y^{(4)} = Q(x)y, \tag{4.5}$$

where $Q(x) > 0$ for $|x| > \delta$ and $Q(x) < 0$ for $|x| < \delta$. In Appendix B, the WKB analysis of (4.5) is carried out. It is shown that the matching process could succeed only if oscillatory components are added at infinity.

5. Conclusions. Previous work on elasto-plastic models has identified two modes of ill-posedness that are characterized by uncontrolled growth of the high frequency modes associated with the plane wave solutions in certain directions. This process will mobilize arbitrarily fine scale deformations that will ultimately violate the continuum assumption on which elasto-plastic models are built. We have proposed an elasto-plastic microstructure model that provides a continuum representation for two additional types of deformations at the microscale. The first accounts for elastic microscale rotations of grains by means of the continuum Cosserat theory proposed by Mindlin and Tiersten [8]. The second represents microscale voiding by means of a dispersive pressure term in the model. The microstructure terms involve the addition of small fourth-order derivatives to the original elasto-plastic model, that have a dispersive effect on the solution. Using both Fourier analysis and energy estimates on the linearized problem, we have shown that the small microstructure terms serve to regularize the solutions to the model equations and inhibit the uncontrolled growth of the highest frequency modes that characterizes ill-posedness. For both types of ill-posedness (shear-band and flutter), we have used matched asymptotics and WKB theory to derive a relationship between the thickness of the localized zone of ill-posedness and the natural length scale of the material.

The analysis in this paper has been essentially linear, exploring the effect of the mobilization of microscale deformations after the onset of ill-posedness. A more complete analysis of the post-critical behavior of the elasto-plastic-micro material requires the inclusion of nonlinear effects and has been explored in another study [3].

Although the reader may find the proof of the energy inequality for strictly hyperbolic equations (cf. Taylor [12] and the references therein) and the theory on higher-order turning point problems (cf. Wasow [15] and the references therein) elsewhere, for the sake of completeness we present a brief derivation of these two results in Appendix A.

Appendix A. On an energy inequality for strictly hyperbolic equations. Consider the first-order hyperbolic system

$$\partial_t u_j = a_{jkl}(x,t)\partial_{x_l} u_k + f_j, \qquad j = 1, \ldots, n.$$

It is said to be strictly hyperbolic if all eigenvalues of the matrix $\{a_{jkl}(x,t)\xi_l\}$ are real and distinct.

When $\{a_{jkl}(x,t)\xi_l\}$ is symmetric, i.e., $a_{jkl}(x,t)\xi_l = a_{kjl}(x,t)\xi_l$, the energy inequality is straightforward. Suppose that $u_j \in C\left(0,T;C_0^1\left(\mathbb{R}^n\right)\right) \cap C^1\left(0,T;C_0\left(\mathbb{R}^n\right)\right)$, $j = 1, \ldots, n$. Then we have

$$\frac{d}{dt}\int_{\mathbb{R}^n} u_j u_j dx = \int_{\mathbb{R}^n} u_j a_{jkl}\partial_l u_k dx + \int_{\mathbb{R}^n} u_j a_{jkl}\partial_l u_k dx + 2\int_{\mathbb{R}^n} f_j u_j dx.$$

Integrating the second term on the right-hand side of the above equation by parts, we obtain

$$\frac{d}{dt}\int u_j u_j dx = \int u_j a_{jkl}\partial_l u_k dx - \int \partial_l u_j a_{jkl} u_k dx - \int \partial_l a_{jkl} u_j u_k dx + 2\int f_j u_j dx,$$

Note that the sum of first two terms on the right-hand side is zero. By the Cauchy inequality,

$$\frac{d}{dt}\|u(\cdot,t)\|_2^2 \le C\left(\|f(\cdot,t)\|_2^2 + \|u(\cdot,t)\|_2^2\right),$$

where $\|u\|_2^2 = \int |u(x,t)|^2 dx$. It follows from Gronwall's inequality that

$$\|u(\cdot,t)\|_2^2 \le C\left(\|u(\cdot,0)\|_2^2 + \int_0^t \|f(\cdot,\tau)\|_2^2 d\tau\right).$$

However, when $\{a_{jkl}(x,t)\xi_k\}$ is not symmetric, the above proof is not valid. A symmetrizer, which not only depends on (x,t) but also depends on the direction ξ in the Fourier space, must be constructed. Suppose that $\lambda_1(x,t,\xi) < \lambda_2(x,t,\xi) < \cdots < \lambda_n(x,t,\xi)$ are eigenvalues of the matrix $A = \{a_{jkl}(x,t)\xi_l\}$, which are homogeneous of degree one in ξ. The projections onto the associated eigenvalues of $\lambda_j(x,t,\xi)$ are given by

$$P_j = \frac{1}{2\pi i}\oint_{C_j} \frac{dz}{zI - A(x,t,\xi)},$$

where C_j is a closed curve containing λ_j. Let $R(x,t,\xi) = \sum_{j=1}^n P_j(x,t,\xi)^T P_j(x,t,\xi)$. It is easy to see that R is positive definite, homogeneous of degree zero in ξ, and $RA = AR$. In the theory of pseudodifferential operators [12], an operator is defined by

$$p(x,D)u = \int e^{2\pi i(x,\xi)} p(x, 2\pi i\xi)\hat{u}(\xi)\, dx, \tag{A.1}$$

where $\hat{u}$ is the Fourier transform of u. When p is a polynomial of D, (A.1) coincides with the corresponding differential operator. Now we estimate the integral

$\int (Ru)_j (x,t)\, u_j (x,t)\, dx$:

$$\begin{aligned}
&\frac{d}{dt}\int R_{mj}(x,t,D)\, u_m(x,t)\, u_j(x,t)\, dx \\
&= \int (\partial_t R_{mj} u_m)\, u_j dx + \int (R_{mj}\partial_t u_m)\, u_j dx + \int (R_{mj}u_m)\, \partial_t u_j dx \\
&= \int (R_{mj} a_{mkl}\partial_l u_k)\, u_j dx + \int (R_{mj}u_m)\, a_{jkl}\partial_l u_k dx \\
&\quad + \int (\partial_t R_{mj} u_m)\, u_j dx + \int (R_{mj} f_m)\, u_j dx + \int (R_{mj}u_m)\, f_j dx \\
&= \int (R_{mj} a_{mkl}\partial_l u_k)\, u_j dx - \int a_{jkl}\partial_l (R_{mj}u_m)\, u_k dx - \int (R_{mj}u_m)\, \partial_l a_{jkl} u_k dx \\
&\quad + \int (\partial_t R_{mj} u_m)\, u_j dx + \int (R_{mj} f_m)\, u_j dx + \int (R_{mj}u_m)\, f_j dx.
\end{aligned}$$

Note that, since $RA = AR$, the following inequality holds:

$$\left| \int (R_{mj} a_{mkl}\partial_l u_k)\, u_j dx - \int a_{jkl}\partial_l (R_{mj}u_m)\, u_k dx \right| \le C \int |u(x,t)|^2 dx.$$

Together with the Cauchy inequality, we have

$$\frac{d}{dt}\int (Ru)_j\, u_j dx \le C\left(\|u(\cdot,t)\|_2^2 + \|f(\cdot,t)\|_2^2\right).$$

Using Gronwall's inequality and Gårding's inequality, we obtain

$$\|u(\cdot,t)\|_2^2 \le C\left(\|u(\cdot,0)\|_2^2 + \int_0^t \|f(\cdot,\tau)\|_2^2 d\tau\right).$$

Appendix B. The WKB analysis in the nongeneric case $\eta = \zeta$. In this appendix, we shall carry out an asymptotic analysis of the following two turning point problem:

(B.1) $$\epsilon^4 y^{(4)} = Q(x)y \text{ on } R \text{ and } y(\pm\infty) \text{ being bounded},$$

where $Q(x) < 0$ for $x \in (A,B)$ and $Q(x) > 0$ for $x \notin (A,B)$. The analysis of a similar two turning point problem

$$\epsilon^2 y'' = Q(x)y \text{ on } R \text{ and } y(\pm\infty) \text{ being bounded}$$

with Q satisfying the same properties as above, can be found in [5].

To complete an asymptotic matching near a turning point, it is necessary to find asymptotic behavior as $x \to \pm\infty$ of the Hyperairy equation:

$$y^{(4)} = xy.$$

By studying the integral representation of its solutions and using the method of steepest descent, we can show that, as $x \to +\infty$,

$$
\begin{aligned}
J_1 &\sim \frac{x^{-3/8}}{2\sqrt{2\pi}} \exp\left(-\frac{4}{5}x^{5/4}\right), \\
J_2 &\sim \frac{x^{-3/8}}{\sqrt{2\pi}} \sin\left(\frac{\pi}{4} + \frac{4}{5}x^{5/4}\right), \\
J_3 &\sim \frac{x^{-3/8}}{\sqrt{2\pi}} \cos\left(\frac{\pi}{4} + \frac{4}{5}x^{5/4}\right), \\
J_4 &\sim \frac{x^{-3/8}}{\sqrt{2\pi}} \exp\left(\frac{4}{5}x^{5/4}\right),
\end{aligned} \tag{B.2}
$$

and, as $x \to -\infty$,

$$
\begin{aligned}
J_1 &\sim \frac{|x|^{-3/8}}{\sqrt{2\pi}} \left[\exp\left(\frac{2\sqrt{2}}{2}|x|^{5/4}\right) \sin\left(\frac{\pi}{8} + \frac{2\sqrt{2}}{5}|x|^{5/4}\right)\right. \\
&\quad \left. + \exp\left(-\frac{2\sqrt{2}}{2}|x|^{5/4}\right) \sin\left(\frac{\pi}{8} + \frac{2\sqrt{2}}{5}|x|^{5/4}\right)\right], \\
J_2 &\sim -\frac{|x|^{-3/8}}{\sqrt{2\pi}} \exp\left(\frac{2\sqrt{2}}{2}|x|^{5/4}\right) \sin\left(\frac{\pi}{8} + \frac{2\sqrt{2}}{5}|x|^{5/4}\right), \\
J_3 &\sim \frac{|x|^{-3/8}}{\sqrt{2\pi}} \exp\left(\frac{2\sqrt{2}}{2}|x|^{5/4}\right) \cos\left(\frac{\pi}{8} + \frac{2\sqrt{2}}{5}|x|^{5/4}\right), \\
J_4 &\sim \frac{|x|^{-3/8}}{\sqrt{2\pi}} \left[\exp\left(\frac{2\sqrt{2}}{2}|x|^{5/4}\right) \cos\left(\frac{\pi}{8} + \frac{2\sqrt{2}}{5}|x|^{5/4}\right)\right. \\
&\quad \left. + \exp\left(-\frac{2\sqrt{2}}{2}|x|^{5/4}\right) \cos\left(\frac{\pi}{8} + \frac{2\sqrt{2}}{5}|x|^{5/4}\right)\right].
\end{aligned} \tag{B.3}
$$

To find the solutions of problem (B.1), we start from the interval $I = (B, +\infty)$. Using the WKB solution, the fact that $Q(x) > 0$, and the requirement that $y(+\infty)$ is bounded, it follows that

$$
y_I = C_1 Q^{-3/8} \exp\left(-\frac{1}{\epsilon}\int_0^x Q^{1/4} dt\right) + C_2 Q^{-3/8} \sin\left(-\frac{1}{\epsilon}\int_0^x Q^{1/4} dt + \varphi_0\right).
$$

Using (B.2) and (B.3) to perform asymptotic matching near B, we can find a formula in the interval $\mathrm{II} = (A, B)$:

$$
\begin{aligned}
y_{\mathrm{II}} = (-Q)^{-3/8} &\left\{2C_1 \left[\exp\left(\frac{1}{\sqrt{2}\epsilon}\int_x^B (-Q)^{1/4} dt\right) \sin\left(\frac{\pi}{8} + \frac{1}{\sqrt{2}\epsilon}\int_x^B (-Q)^{1/4} dt\right)\right.\right. \\
&\left. + \exp\left(-\frac{1}{\sqrt{2}\epsilon}\int_x^B (-Q)^{1/4} dt\right) \sin\left(\frac{3\pi}{8} + \frac{1}{\sqrt{2}\epsilon}\int_x^B (-Q)^{1/4} dt\right)\right] \\
&\left. - C_2 \exp\left(\frac{1}{\sqrt{2}\epsilon}\int_x^B (-Q)^{1/4} dt\right) \sin\left(\frac{3\pi}{8} + \frac{1}{\sqrt{2}\epsilon}\int_x^B (-Q)^{1/4} dt - \varphi_0\right)\right\}.
\end{aligned}
$$

Similarly, if the matching starts from the left interval $(-\infty, A)$, we obtain another formula in the interval $\mathrm{II} = (A, B)$:

$$y^*_{\mathrm{II}} = (-Q)^{-3/8}\left\{2C_1^*\left[\exp\left(\frac{1}{\sqrt{2}\epsilon}\int_A^x(-Q)^{1/4}dt\right)\sin\left(\frac{\pi}{8}+\frac{1}{\sqrt{2}\epsilon}\int_A^x(-Q)^{1/4}dt\right)\right.\right.$$
$$\left.+\exp\left(-\frac{1}{\sqrt{2}\epsilon}\int_A^x(-Q)^{1/4}dt\right)\sin\left(\frac{3\pi}{8}+\frac{1}{\sqrt{2}\epsilon}\int_A^x(-Q)^{1/4}dt\right)\right]$$
$$\left.-C_2^*\exp\left(\frac{1}{\sqrt{2}\epsilon}\int_A^x(-Q)^{1/4}dt\right)\sin\left(\frac{3\pi}{8}+\frac{1}{\sqrt{2}\epsilon}\int_A^x(-Q)^{1/4}dt-\varphi_0^*\right)\right\}.$$

The equality $y_{\mathrm{II}} \equiv y^*_{\mathrm{II}}$ requires

$$2C_1^*\sin\left(\frac{3\pi}{8}+\frac{1}{\sqrt{2}\epsilon}\int_A^x(-Q)^{1/4}dt\right)-C_2\exp\left(\frac{1}{\sqrt{2}\epsilon}\int_A^B(-Q)^{1/4}dt\right)$$
$$\cdot\sin\left(\frac{1}{\sqrt{2}\epsilon}\int_A^x(-Q)^{1/4}dt-\frac{1}{\sqrt{2}\epsilon}\int_A^B(-Q)^{1/4}dt-\frac{3\pi}{8}+\varphi_0\right)$$
$$+2C_1\exp\left(\frac{1}{\sqrt{2}\epsilon}\int_A^B(-Q)^{1/4}dt\right)$$
$$\cdot\sin\left(\frac{1}{\sqrt{2}\epsilon}\int_A^x(-Q)^{1/4}dt-\frac{1}{\sqrt{2}\epsilon}\int_A^B(-Q)^{1/4}dt-\frac{\pi}{8}\right)\equiv 0,$$
$$2C_1^*\sin\left(\frac{\pi}{8}+\frac{1}{\sqrt{2}\epsilon}\int_A^x(-Q)^{1/4}dt\right)+2C_1\exp\left(-\frac{1}{\sqrt{2}\epsilon}\int_A^B(-Q)^{1/4}dt\right)$$
$$\cdot\sin\left(\frac{1}{\sqrt{2}\epsilon}\int_A^x(-Q)^{1/4}dt-\frac{1}{\sqrt{2}\epsilon}\int_A^B(-Q)^{1/4}dt-\frac{3\pi}{8}\right)$$
$$-C_2^*\sin\left(\frac{3\pi}{8}+\frac{1}{\sqrt{2}\epsilon}\int_A^x(-Q)^{1/4}dt-\varphi_0^*\right)\equiv 0.$$

The following conditions should, therefore, be satisfied:

$$\frac{1}{\sqrt{2}\epsilon}\int_A^B(-Q)^{1/4}dt+\frac{\pi}{2}\sim n\pi,\quad \frac{\pi}{4}-\varphi_0=m\pi,\quad \frac{\pi}{4}-\varphi_0^*=k\pi,$$

and

$$(-1)^n(2C_1-C_2)\exp\left(\frac{1}{\sqrt{2}\epsilon}\int_A^B(-Q)^{1/4}dt\right)+2C_1^*=0,$$
$$(-1)^n 2C_1\exp\left(-\frac{1}{\sqrt{2}\epsilon}\int_A^B(-Q)^{1/4}dt\right)+(2C_1^*-C_2^*)=0,$$

where m, n, and k are integers.

Acknowledgment. Lianjun An is grateful to Professor Chadam for his sponsorship of this research program at McMaster and for his continuing encouragement.

REFERENCES

[1] L. AN, *Loss of hyperbolicity in elastic-plastic material at finite strains*, SIAM J. Appl. Math., 54 (1993), pp. 621–654.
[2] ———, *The genericity of flutter ill-posedness in 3-dimensional elastic-plastic models*, Quart. Appl. Math., (1993), to appear.
[3] L. AN AND A. PEIRCE, *A weakly nonlinear analysis of elasto-plastic-microstructure models*, SIAM J. Appl. Math., Submitted.
[4] L. AN AND D. SCHAEFFER, *The flutter instability in granular flow*, J. Mech. Phys. Solids, 40 (1992), pp. 683–698.
[5] C.M. BENDER AND S.A. ORSZAG, *Advanced Mathematical Methods for Scientists and Engineers*, McGraw-Hill, New York,, 1978.
[6] B. LORET, *Does deviation from deviatoric associativity lead to the onset of flutter instability*, 1991, preprint.
[7] J. MANDEL, *Condition de stabilité et postulat de Drucker*, Rheology and Soil Mechanics, J. Kravtchenko and P. Sirieys, eds., IUTAM Symposium at Grenoble, Springer-Verlag, 1966, pp. 58–68.
[8] R.D. MINDLIN AND H.F. TIERSTEN, *Effects of couple-stresses in linear elasticity*, Arch. Rational Mech. Anal., 11 (1962), pp. 415–448.
[9] H.-B. MÜHLHAUS AND I. VARDOULAKIS, *The thickness of shear bands in granular materials*, Géotechnique, 37 (1987), pp. 271–283.
[10] J. RICE, *The localization of plastic deformation*, Proc. 14th IUTAM Congress, W. Koiter, ed., Delft, the Netherlands, 1976, pp. 207–220.
[11] D. SCHAEFFER, *Instability and ill-posedness in the deformation of granular materials*, Internat. J. Numer. Anal. Mech. Geomech, 14 (1990), pp. 253–278.
[12] M. TAYLOR, *Pseudo Differential Operators*, Springer-Verlag, New York, 1974.
[13] R.A. TOUPIN, *Elastic materials with couple-stresses*, Arch. Rational Mech. Anal., 11 (1962), pp. 385–414.
[14] I. VARDOULAKIS AND E.C. AIFANTIS, *Gradient dependent dilatancy and its implications in shear banding and liquefaction*, Ingenieur-Archiv, 59 (1989), pp. 197–208.
[15] W. WASOW, *Linear Turning Point Theory*, Springer-Verlag, New York, 1985.